Sorption and Transport of Water Vapor in Films of Alginic Acid, Sodium Alginate, and Alginate-Cobalt Complex with Three Different Uronic Acid Compositions (Commemoration Issue Dedicated to Professor Hisashi Odani On the Occasion of His Retirement)

AUTHOR(S):

Hirai, Asako; Odani, Hisashi

Bull. Inst. Chem. Res., Kyoto Univ., Vol. 70, No. 2, 1992

Sorption and Transport of Water Vapor in Films of Alginic Acid, Sodium Alginate, and Alginate-Cobalt Complex with Three Different Uronic Acid Compositions.

Asako HIRAI* and Hisashi ODANI*

Received July 13, 1992

The sorption and transport of water vapor were studied for films of alginc acid (AGA), sodium alginate (AGNa), and alginate-cobalt complex (AGCo) having three different uronic acid compositions, the M/G ratios. Sorption isotherms for all films of AGA, AGNa, and AGCo were of Type II isotherm of the Brunauer classification. These isotherms were not affected by differences in the M/G ratios of films. The integral absorption from and desorption to zero pressure exhibited non-Fickian characteristic features for all films. The mean permeability coefficient $\bar{P}(C)$ showed pressure dependence, especially in the low vapor pressure region. $\bar{P}(C)$ for AGNa was higher than that for AGA, which results from greater hygroscopic nature of AGNa than AGA. In contrast $\bar{P}(C)$ for AGCo was much lower than that for AGA at lower pressures and it approached to that for AGA in higher vapor pressure region. This was interpreted as the strong interaction between water and the complex film. Integral diffusion coefficient $\bar{D}$(C) evaluated as $\bar{P}(C)/S$ (C), where the solubility coefficient $S(C)$ is estimated from the sorption isotherms, increased rapidly with increasing concentration and then leveled off at higher concentrations. No difference was observed in $\bar{D}(C)$ between H_2O-AGA and H_2O-AGNa systems at the same concentrations. However, appreciable difference in $\bar{D}(C)$ between H_2O-AGA and H_2O-AGCo was observed; in the low and medium concentration regions $\bar{D}(C)$ for AGA were much higher than that for AGCo.

KEYWORDS: Absorption and desorption/ Permeation/ Permeability coefficient/ Diffusion coefficient/ Water vapor/ Alginic acid/ Sodium alginate/ Alginate-cobalt complex/ b-D-Mannuronic acid residue/ a-L-Guluronic acid residue

INTRODUCTION

Alginic acid is known[1] as a linear polysaccharide of (1→4) linked b-D-mannuronic acid, M, and a-L-guluronic acid, G, residues arranged in a non-regular, blockwise fashion along the chain. That is, the chain is composed of M-block including only M residues, G-block including only G residues, and MG-heteroblock including M and G residues. The chain conformations of M-block and G-block were suggested to be "flat-ribbon" and "buckled-ribbon" forms,[2,3] respectively. Since both conformations are drastically different

* 平井諒子, 小谷 壽: Laboratory of Fundamental Material Properties, Institute for Chemical Research, Kyoto University, Uji, Kyoto 611.

from each other, the physical properties of alginates depend not only upon the uronic acid composition (M/G ratio) but also upon the relative proportion of three types of blocks.

In a previous report[4] we have examined the sorption and transport of water vapor in films of alginic acid, sodium alginate and alginate-cobalt complex of G-rich samples. This paper describes the sorption and transport behavior of water vapor in films prepared from M-rich and NB samples, where the latter sample contains nearly equal amount of M and G residues. The behavior for M-rich and NB samples will be compared with that for G-rich sample and discussed in terms of their crystalline structures.

FUNDAMENTALS

The permeation of gases through a nonporous polymer membrane is governed by the coupled solution-diffusion mechanism.[5] The gas molecules dissolve in the surface layer on the ingoing side of the membrane, diffuse across the membrane in response to the concentration gradient, and evaporate from the other surface on the outgoing side.

Data usually obtained from permeation measurements are the amount of gas, Q_t, which has passed through unit area of the membrane for a time t. A plot of Q_t versus t is called the permeation curve. As shown in Figure 1, the permeation curve is convex toward the

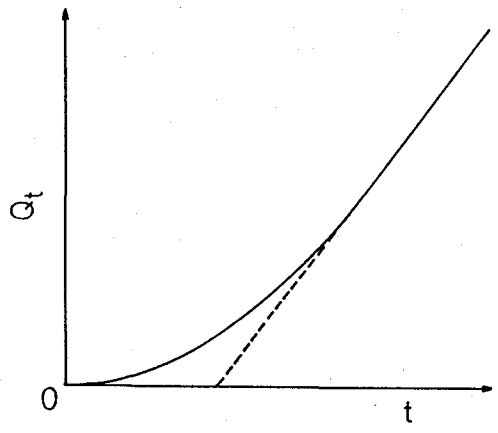

Figure 1. Typical permeation curve.

time axis at short times and then approaches a straight line as t increases. Permeation is in the steady state on the asymptotic linear portion of the permeation curve, since the rate of permeation is independent of time. In the steady state the concentration remains constant at all points of the membrane.

Theoretical relations necessary for the analysis of data obtained from isothermal permeation measurements with a membrane, where diffusion occurs effectively in one direction x, are obtained from solutions of the Fick diffusion equation,

$$\frac{\partial C}{\partial t}=\left(\frac{\partial}{\partial x}\right)\left[D\left(\frac{\partial C}{\partial x}\right)\right], \tag{1}$$

subject to appropriate initial and boundary conditions. Here, C is the concentration of penetrant and D is the mutual diffusion coefficient of the system.

At the beginning of a permeation experiment the concentration is uniform everywhere in the membrane. This initial concentration is denoted by C_0. Then we have

$$C=C_0, \qquad 0<x<X, \; t=0, \tag{2}$$

where X is the thickness of the membrane. The origin of x is taken at the surface on the ingoing side. The boundary condition for $x=0$ is

$$C=C_\infty , \qquad x=0, \; t>0, \tag{3}$$

where C_∞ denotes the equilibrium concentration corresponding to the pressure on the ingoing side, p_∞ . If the swelling of the membrane during permeation is ignored, we may write

$$C=C_0, \qquad x=X, \; t>0. \tag{4}$$

Analytic solutions to Eq. (1) subject to these conditions can be obtained only for the special case in which D is independent of C.[6] When D is constant, Q_t under the conditions of Eqs. (2)−(4) and $C_\infty \gg C_0 \simeq 0$, is given by

$$\frac{Q_t}{XC_\infty}=\frac{D_0 t}{X^2}-\frac{1}{6}-\frac{2}{\pi^2}\sum_{n=1}^{\infty}\frac{(-1)^n}{n^2}\exp\left(-\frac{D_0 n^2 \pi^2 t}{X^2}\right), \tag{5}$$

where D_0 denotes constant D. As t goes to infinity, the steady state is approached and the exponential terms become negligibly small, so that the plot of Q_t versus t tends to a line as shown in Figure 1,

$$Q_t=\frac{D_0 C_\infty}{X}\left(t-\frac{X^2}{6D_0}\right). \tag{6}$$

The steady-state permeation rate, J_s, is mathematically defined by

$$J_s=\lim_{t\to\infty}\frac{dQ_t}{dt} \tag{7}$$

In view of Eq. (6), J_s is related to D_0 by the equation

$$J_s=D_0 C_\infty / X. \tag{8}$$

The relation between C_∞ and the corresponding pressure p_∞ is given by an expression of the form

$$C_\infty=S\, p_\infty , \tag{9}$$

where S is the solubility coefficient of the gas in the polymer. When Henry's law is obeyed,

this is usually the case for systems of a simple gas and rubbery polymer, S is independent of concentration, or pressure, i.e. $S=S_0$, a constant. Then J_s can be expressed as

$$J_s=D_0\,S_0\,p_\infty\,/\,X \tag{10}$$

or

$$P_0\equiv D_0\,S_0=J_s\,X\,/\,p_\infty\,. \tag{11}$$

The product $P_0\equiv D_0\,S_0$ is referred to the permeability constant. The value of P_0 is thus determined from the slope of the linear portion of the permeation curve.

For systems in which D is a function of concentration alone, that is, for Fickian system, we can deduce necessary relations to analyze permeation data without recourse to actual calculations. For a Fickian system, Eq. (8) is experssed as[7,8]

$$J_s(C_\infty)=\bar{D}(C_\infty)\,C_\infty\,/X. \tag{12}$$

Here $\bar{D}(C_\infty)$ is the quantity called the integral diffusion coefficient for the concentration C_∞, and is defined by

$$\bar{D}(C_\infty)=\frac{1}{C_\infty}\int_0^{C_\infty} D(C)\,\mathrm{d}C. \tag{13}$$

For Fickian systems, nonlinear sorption isotherms are frequently observed. In these cases, the solubility coefficient is a function of concentration (or pressure); that is $S=S\,(C_\infty)$. Using the concentration-dependent $S(C_\infty)$ we obtain from Eq. (12) the relation

$$\bar{P}(C_\infty)\equiv\bar{D}(C_\infty)\,S(C_\infty)=J_s(C_\infty)\,X\,/\,p_\infty\,. \tag{14}$$

$\bar{P}$ is referred to the (mean) permeability coefficient.

The ordinary method of determining the solubility and the diffusion coefficients is to measure the rates of absorption and desorption of penetrant in polymer. If the diffusion coefficient is not constant or depends only on C, but depends on t or x, however, value of D is not easily estimated from the absorption and desorption behavior. Even in this case, the data of S and $\bar{P}$, which have been determined, respectively, from sorption and permeation measurements at various pressures, in Eq. (14) yields $\bar{D}$ as a function of concentration. This in turn allows determination of the mutual diffusion coefficient D as a function C.[6,8] This procedure contains no approximation other than the neglect of the change in membrane thickness due to swelling and applies in circumstances in which D is time-dependent or the condition of constant surface concentration is not obeyed; that is, absorption-desorption behavior is non-Fickian.

EXPERIMENTAL

Materials

Two kinds of commercial sodium alginates, being respectively rich in mannuronate, M, and guluronate, G, components, were supplied by Kimitsu Chemicals Co. Sample NB which contains nearly equal amount of M and G was purchased from Nacalai Tesque, INC. Each alginate was purified by the following procedure: The dry material (8 g) was added little by little to 130 ml of the cold solution of 2 wt% hydrochloric acid and stirred for 1 hr and filtered off. The precipitate was treated further twice in the same procedure. The precipitate was neutralized with cold distilled water, washed with ethanol and then dried *in vacuo*. The weighed amount of the product (alginic acid) thus obtained was suspended in distilled water and dissolved completely by adding of equivalent mole of dilute sodium hydroxide solution. The sodium alginate was finally isolated by reprecipitation with ethanol, washed with 50wt% ethanol-water solution and dried *in vacuo*.

Each sodium alginate film AGNa from three kinds of samples (M1Na, G1Na, and NBNa) was prepared by casting 2 wt% aqueous solution of purified sodium alginate on the glass plate and evaporating water at room temperature. Alginic acid film AGA (M1, G1, and NB) was prepared by neutralizing the sodium alginate film with 2 wt% HCl in 50wt% ethanol-water solution, washed with 50wt% ethanol-water solution, and then immersed in methanol, and dried in air. Alginate-cobalt complex film AGCo (M1Co, G1Co and NBCo) was prepared by immersion of the sodium alginate film in 0.05 M $CoSO_4$ 30 wt% ethanol-water solution, and washed with 30 wt% ethanol-water solution and then washed with water and dried in air.

The film thickness was determined by taking the arithmetic average of numerous readings of a micrometer screw gauge over the area of the film. The films of 17-21 μm thick were used. The density was determined from the known weight, area and thickness of the film.

Water vapor used as a penetrant was evolved from deionized water, which had been degassed at least three times before the experiments.

NMR measurements

Each sodium alginate (0.1 g) was dissolved in 2 ml D_2O at 40°C, and placed in a 10 mmϕ NMR test tube. 100 MHz ^{13}C NMR spectra were recorded with JEOL JNM-GX 400 spectrometer using 9.4T, 45° pulse, pulse repetition time of 4 s, and 27,000-30,000 scans, at 70°C.

X-ray diffraction analysis

X-ray diffraction patterns for alginic acid films were obtained using Cu-Kα radiation monochromatized by graphite single crystal. As an X-ray source, a rotating anode X-ray generator, Rigaku Denki Rotaunit RU-3H was used, operated at 40 kV and 80 mA. The film of about 20 μm thick was cut into 1 mm×15 mm strips and the strips thus obtained were piled up to the thickness of about 0.3 mm with their long axis aligned parallel to one another. The long axis of the strips was set vertically. The incident direction of X-ray was parallel to the film surface. The X-ray camera and the sample were set in the vacuum with

a bottle full of water. The vacuum chamber was first evacuated by aspirator, then cut off the suction, and kept during the measurement at 18°C. Hence the vapor pressure of water remained constant during measurement in the chamber. The *d*-spacing of (111) of $CaCo_3$, 3.0356 Å, was used to calibrate the camera length.

Absorption and desorption measurements

The absorption and desorption experiments were carried out by the weighing method. The amount of water at absorption equilibrium and the rates of absorption and desorption were measured using a high-vacuum apparatus equipped with an electromagnetic microbalance (Model GAB-1, Chyo Balance Corp.). The pressure of water vapor was measured with a Baratron pressure transducer (Type 221A, MKS). Integral absorption from, and desorption to, zero concentration were measured at 30°C.

Permeation measurements

The transmission of water vapor through the films was determined by the cup method as shown in Figure 2. The glass vessel with a saturated salt solution to obtain a given vapor pressure were put in the aluminum cup. The film fixed with paraffin in a frame was dried *in vacuo* and attached to the aluminum cup. Then, the cup equipped with the film and the salt solution was immediately put in a desiccator maintained zero vapor pressure at 30°C with desiccant of P_2O_5. The transmission of water vapor was determined from a decrease in weight of the cup.

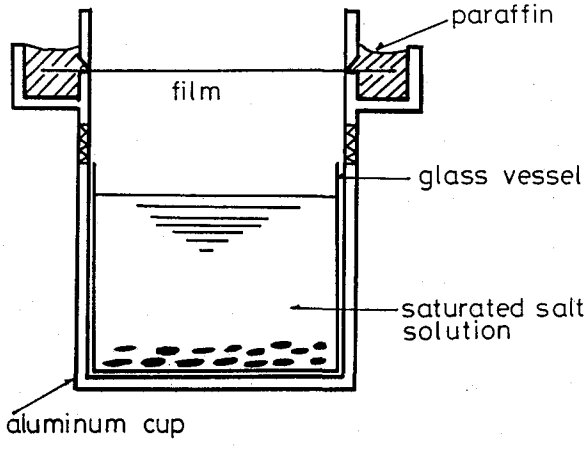

Figure 2. The cup method for permeation experiment.

RESULTS AND DISCUSSION

Figure 3 shows the 100 MHz ^{13}C NMR spectra for three alginate samples in D_2O at 70°C. All the assignments of spectra were made after Grasdalen et al.[9,10] From these spectra the M/G ratios and diad frequencies were obtained as shown in Table I by the previous-

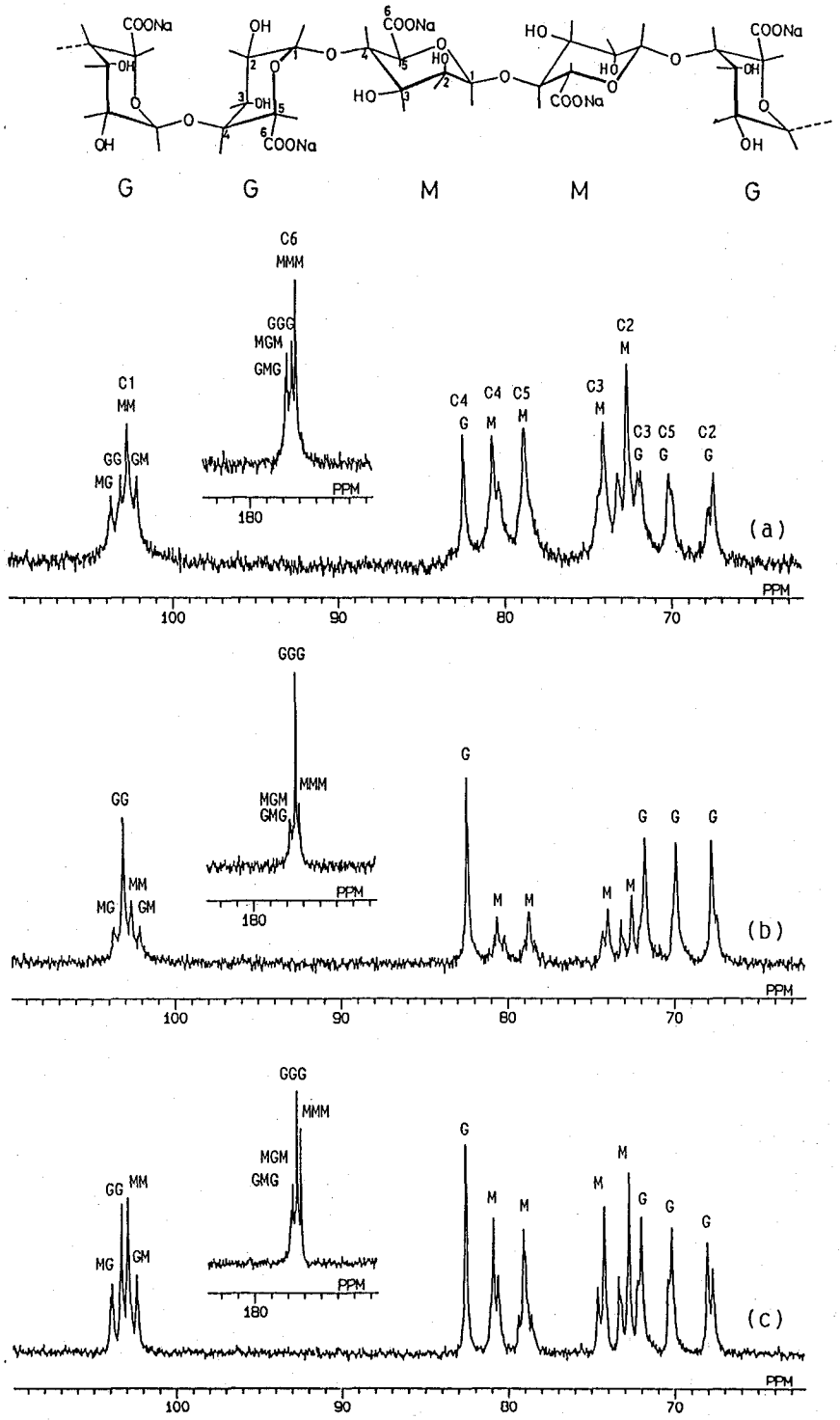

Figure 3. 100 MHz ^{13}C NMR spectra of sodium alginate in D_2O at 70°C: (a) M1Na, (b) G1Na, and (c) NBNa.

Table I M/G ratios and diad frequencies for AGNa determined from ^{13}C NMR spectra

sample	M/G ratio	F_{MM}	F_{MG}, F_{GM}	F_{GG}
M1Na	1.78	0.47	0.17	0.19
G1Na	0.56	0.22	0.14	0.50
NBNa	1.08	0.34	0.18	0.30

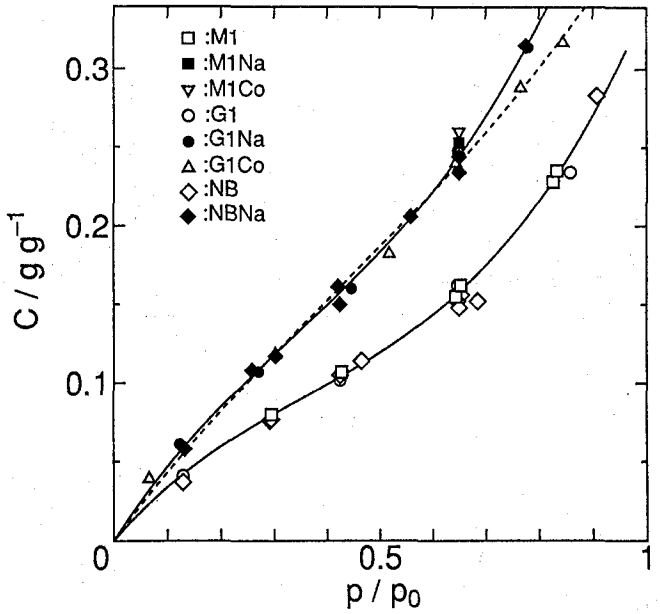

Figure 4. Sorption isotherms of water vapor in alginic acid films M1, G1, NB, sodium alginate films M1Na, G1Na, NBNa, and alginate-cobalt complex films M1Co, and G1Co at 30°C. □: M1, ○: G1, ◇: NB, ■: M1Na, ●: G1Na, ◆: NBNa, ▽: M1Co, △: G1Co.

ly reported method.[11] Figure 3 and Table I demonstrate that sample M1Na is rich in MM and MMM, and that sample G1Na is rich in GG and GGG. NBNa sample has nearly equal amount of MM and GG, and is rich in MMM and GGG. The portion of homopolymeric sequences is larger than strictly alternating MG sequences.

Figure 4 shows the sorption isotherms of water vapor at 30°C in films of alginic acid, sodium alginate, and alginate-cobalt complex having three different M/G ratios. Alginic acid film, sodium alginate film and alginate-cobalt complex film prepared from M-rich sample are designated as M1, M1Na, and M1Co, respectively. Films prepared from G-rich sample are designated as G1, G1Na, and G1Co in a manner similar to M-rich sample. Films prepared from sample NBNa(M/G=1.08) are designated as NB, NBNa and NBCo. C is the concentration of water absorbed by dry polymer at equilibrium and p and p_0 are the pressure and the saturated pressure of water vapor, respectively. The data from different samples fall satisfactorily on respective curves. Sorption isotherms for all films of AGA, AGNa, and AGCo are of the type II isotherm of the Brunauer classification.[12] The amount of water at

sorption equilibrium for sodium alginate films is higher than that for alginic acid films in the whole pressure range studied. This is ascribed to the stronger interaction between the carboxylate anions in sodium alginate molecules and water. The amount of water at sorption equilibrium for alginate-cobalt complex films is almost the same as that for sodium alginate films in the region below $p/p_0=0.65$, but is lower above 0.65. Sodium alginate films are soluble in water, while sodium alginate-cobalt complex films are insoluble in water because the degree of swelling is depressed by the complex formation between the carboxylate anions in sodium alginate molecules and Co^{++} ions. For all films of AGA, AGNa, and AGCo these sorption isotherms were not affected by differences in the M/G ratios. This might be due to the fact that M and G residues have the same number of hydrophilic groups as described below. In the case of alginate-cobalt complex films, however, it should be considered how the Co^{++} ion works in water sorption behavior. It was shown by Cozzi et al.[13,14] that the amount of divalent ions to obtain precipitation of alginates increases in the order of Pb, Cu<Ca<Co, Ni, Zn<Mn. The ion exchange properties of alginates were found to depend on the M/G ratio of the alginate. In the cases of Pb, Cu and Ca, M-rich alginates had a lower affinity to these divalent ions in ion exchange reactions than G-rich alginates. For metals with low affinity, like cobalt, however, this different behavior was not so pronounced; that is, there was little difference in affinities for Co^{++} ion with alginates between G-rich alginate and M-rich alginate. In our atomic absorption analysis, the same amount of cobalt ion is contained in Co-complex films with three different M/G ratios as shown in Table II. This result corresponds well to the results obtained by Cozzi et al. summarized above. Almost the same amount of water is absorbed for three samples at the same pressure.

Table II The amount of water at sorption equilibrium and the content of Co in alginate-cobalt complex films.

sample	p/p_0	C/g g^{-1}	mole of Co per monomer unit[a]
G1Co	0.65	0.24	0.31
M1Co	0.65	0.26	0.31
NBCo	0.65	0.24	0.32

a) by atomic absorption analysis

Figure 5 shows data of integral absorptions from and desorptions to zero pressure for alginic acid films of M-rich sample, M1, at 30°C. The integral absorption curves are sigmoid for all pressures studied, and in each run the initial rate of desorption is faster than that of the corresponding sorption. The absorption and desorption curves show pronounced dependences on the relative humidity, i.e. on the concentration.

Figure 6 shows the results of integral absorption and desorption measurements at $p/p_0=0.43$. The results are shown in the forms of the Fickian plots, M_t/M_∞ against $t^{1/2}/X$. Here M_t is the amount of water absorbed by the polymer film or desorbed from the film at time t, M_∞ the final uptake or loss at infinite time, X the thickness of the film. The absorption and desorption curves are non-linear as shown in Figure 6, therefore, the diffusion pro-

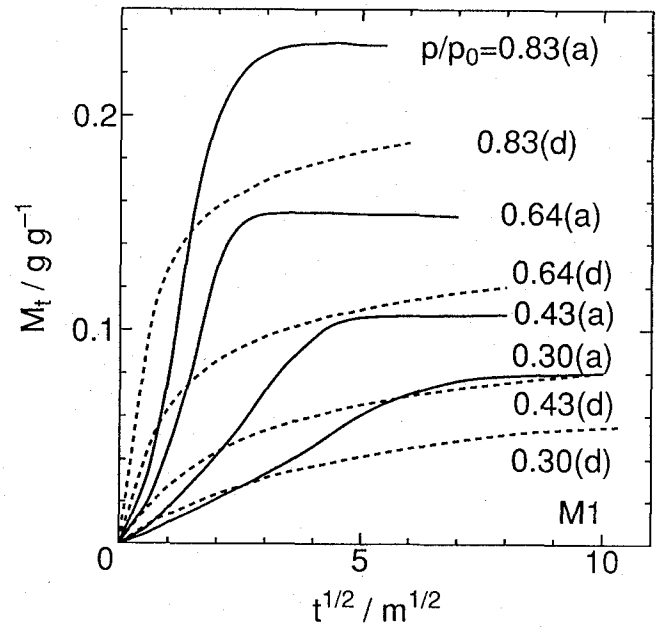

Figure 5. Integral absorptions from and desorptions to zero pressure for alginic acid film M1 as a function of relative humidity at 30°C. Solid line, absorption; Dashed line, desorption.

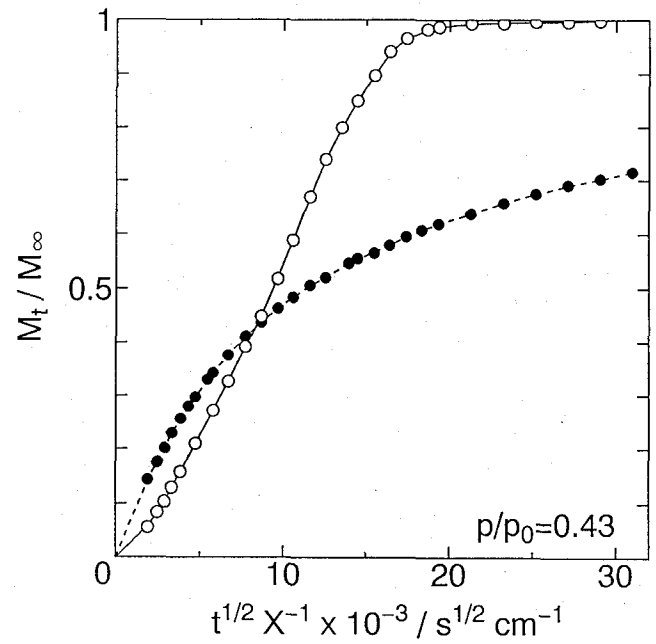

Figure 6. Fickian plots for water vapor in alginic acid film M1 at the relative vapor pressure of 0.43 at 30°C. —○—: absorption, ···●···: desorption.

cesses are not true Fickian type. They all studied in this paper are not ture Fickian. Many experimental results[15] show that when a given polymer-penetrant mixture is in the glassy state, the absorption processes depend not only upon the concentration of penetrant but also upon other factors, e.g. the time. Under such circumstances we are not able to evaluate the mutual diffusion coefficient of a given system by using the method which uses measurements of the initial rate of absorption.

The integral diffusion coefficient $\bar{D}(C)$, however, is obtained from steady-state permeation measurements if the pressure dependence of the permeability coefficient $\bar{P}(C)$ are determined. $\bar{D}(C)$ is deduced from $\bar{P}(C)$ and the solubility coefficient $S(C)$ using relation $\bar{D}(C)=\bar{P}(C)/S(C)$ as mentioned above. The rates of steady-state permeation were obtained by the cup method as illustrated in Figure 2.

Figure 7 shows the results of permeation of the water vapor to the alginic acid films M1 at 30°C. Q is the amount of water vapor which has passed through the film for a time interval t. These permeation curves for water vapor show the linear relation against time t, in which each line pass through the origin. The permeability coefficient is determined from the slope of the permeation curve according to the following equation.

$$\bar{P}(C)=\frac{Q}{t}\cdot\frac{X}{p\,A}$$

Here, X is the thickness of the film, p is the vapor pressure, and A is the surface area of the film through which water vapor passes.

Figure 8 shows pressure dependence of the mean permeability coefficient $\bar{P}(C)$ for water vapor in films M1, M1Na, and M1Co at 30°C. The mean permeability coefficient in-

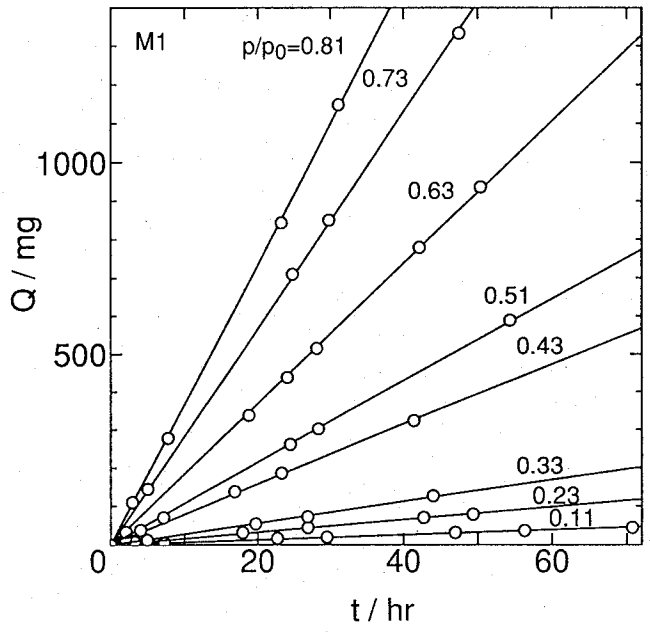

Figure 7. Permeation curves of water vapor for alginic acid film M1 at 30°C at various relative humidities.

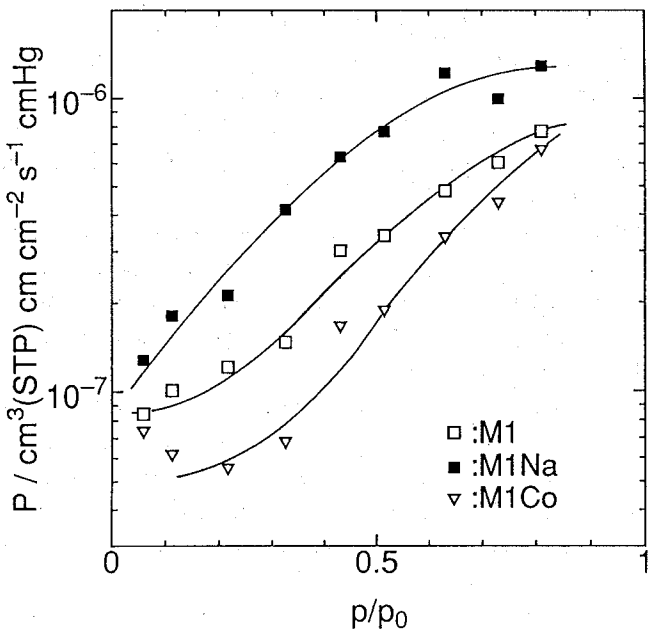

Figure 8. Dependence of mean permeability coefficient for water vapor in films M1, M1Na, and M1Co on relative humidity at 30°C. □: M1, ■: M1Na, ▽: M1Co.

creases with an increase of vapor pressure for every film. $\bar{P}(C)$ for sodium alginate film M1Na is higher than that of alginic acid film M1, This is due to higher hygroscopic nature of sodium alginate film than alginic acid film. Whereas $\bar{P}(C)$ for alginate-cobalt complex film M1Co is lower than that for M1 at lower pressures, it approaches to that for M1 in higher vapor pressure regions ($p/p_0>0.6$). The strong interaction between alginate-cobalt complex film and water is recognized in the region below $p/p_0=0.6$. $\bar{P}(C)$ for other samples are shown in Figure 9 together with those for M1 series. There are no significant differences in $\bar{P}(C)$ among three AGA films with different M/G ratios, and neither for AGNa nor AGCo.

The solubility coefficient $S(C)$ is estimated from sorption isotherms shown in Figure 4. Then the integral diffusion coefficient $\bar{D}(C)$ is calculated using the relation $\bar{D}(C)=\bar{P}(C)$ / $S(C)$. Figure 10 shows the concentration dependence of $\bar{D}(C)$ for the systems H_2O-AGA, H_2O-AGNa, and H_2O-AGCo for different samples at 30°C. The integral diffusion coefficient $\bar{D}(C)$ increases rapidly with an increase of concentration and levels off in all cases. There is no great difference in $\bar{D}(C)$ between H_2O-AGA and H_2O-AGNa systems. Appreciable difference in $\bar{D}(C)$ between H_2O-AGA and H_2O-AGCo is recognized, because of the strong interaction between water and the complex film.

X-ray diffraction patterns of alginic acid films with three different M/G ratios in the presence of water vapor are shown in Figure 11. They show that the chain axis is preferentially oriented parallel to the film surface, though the patterns of three samples are different from each other. All diffraction patterns exhibit low crystallinity and the M1 film is the lowest. To compare their structures, observed d-spacings are tabulated in Table III together

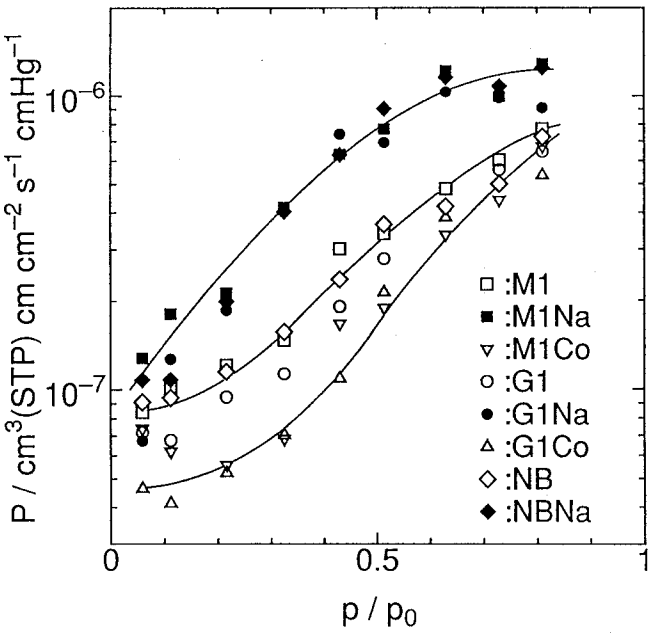

Figure 9. Dependence of mean permeability coefficient for water vapor in alginic acid films M1, G1, NB, sodium alginate films M1Na, G1Na, NBNa and alginate-cobalt complex films M1Co and G1Co on relative humidities at 30°C. □: M1, ○: G1, ◇: NB, ■: M1Na, ●: G1Na, ◆: NBNa, ▽: M1Co, △: G1Co.

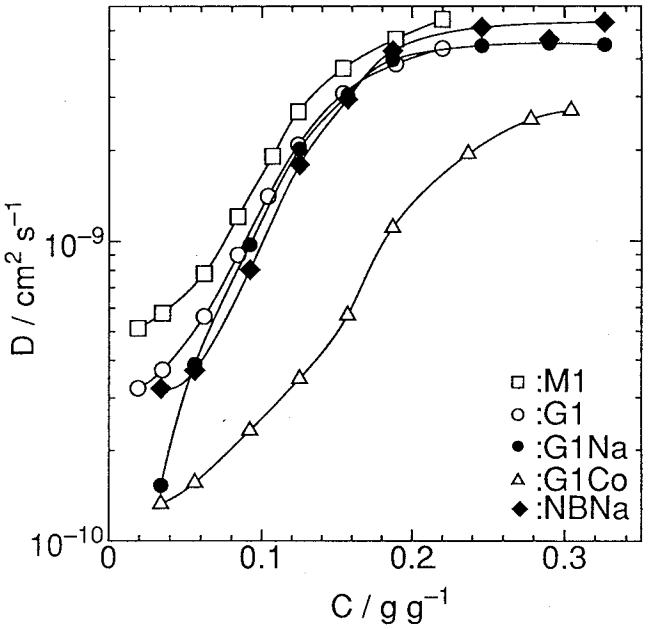

Figure 10. Concentration dependence of integral diffusion coefficient at 30°C. □: M1, ○: G1, ●: G1Na, △: G1Co, ◆: NBNa.

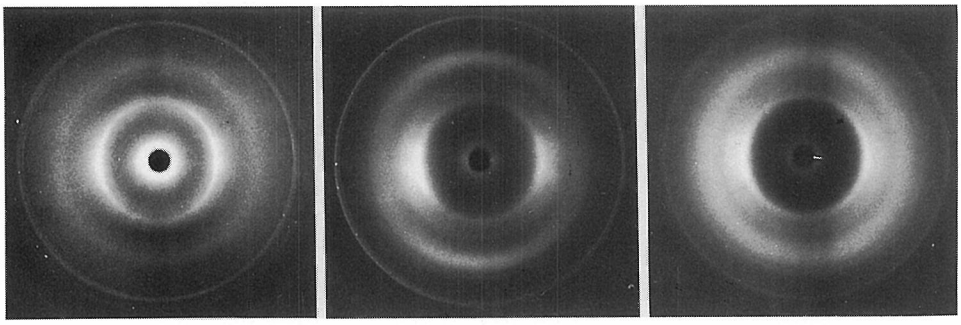

Figure 11. X-ray diffraction patterns of alginic acid films, long axis of the strips is vertical. a: M1, b: G1, c: NB.

Table III The *d*-spacings of M1, G1, and NB films.

d_{obs}			d_{ref}		
			Poly M[a]	Poly G[b]	
M1	G1	NB	wet	wet	dry
6.92−6.24 s	6.99−6.27 s	6.87−6.34 s	6.63(011) w	6.70(101) s	
			5.69(101) m	5.35(002) m	6.23(101)
6.24−5.48 vw	6.27−4.98 m	6.34−4.98 m	5.20(002) m	5.31(111) m	5.30(002)
				4.54(102) m	5.07(111)
			4.45(021) m	4.35(020) s	4.37(102)
			4.30(002) s	4.30(200) vs	4.35(020)
4.24−3.82 m	4.40−3.76 s	4.47−3.79 s	3.80(200) w	4.03(112) m	4.02(021)
				4.02(021) s	3.90(112)
				3.99(201) m	3.85(200)
				3.88(120) s	3.79(120)

[a] Ref. (16)
[b] Ref. (17)

with the *d*-spacings (d_{ref}) of poly-b-D-mannuronic acid (poly M), poly-a-L-guluronic acid (poly G) with water vapor, and poly G in the dry state in the literature.[3,16,17]

Atkins et al.[16,17] reported the crystalline structures of Poly M and Poly G by X-ray diffraction and polarized infrared spectroscopy. The unit-cell dimensions of poly M remained unchanged throughout a wide range of relative humidities (65-100%), although at high humidities (>90%) the reflections tended to be sharper. In the case of poly G the unit-cell dimensions varied with humidity and on intensive drying the reflections became to be broader. Good crystalline order necessitated one water molecule per sugar residue and dehydration resulted in a uniplanar contraction of 1 Å in the *a*-dimension.

The reflections of G1 film can be concluded to come from poly G from the basis of *d*-

spacings and the relative intensities as shown in Table III. Even though the X-ray diagram are very broad, the diffraction pattern of G1 is similar to that of poly G in the literature.[18,19] The diffraction diagram of NB film is also similar to that of G1 and to that of mixture of poly G and M.[18] Though the appearance of the X-ray diagram of M1 is different from those of G1 and NB, the *d*-spacings of M1 seem to come again from poly G. The *d*-spacings of 5.20, and 4.30 Å expected from poly M could not be detected in M1 film and the most inner ring is the strongest so that it may come from poly G. Frei and Preston reported[18] that when the alginic acid was reprecipitated from the mixture of poly M and poly G dissolved as sodium alginate, the precipitate gave an X-ray diagram in which only the inner strong ring of poly G could be clearly recognized. Namely the crystallization of poly G tends to suppress that of poly M.

The G1, M1 and NB films have different M/G ratios, but their crystal parts are almost composed of poly G, which can absorb water vapor, contrary to the crystalline poly M. Their crystallinities are low, and the differences among them are not so significant as observed from Figure 11. Therefore, the sorption behavior of AGA is considered to be essentially correlated with the number of OH and COOH groups. b-D-Mannuronic acid and its C-5 epimer a-L-guluronic acid have the same number of hydrophilic groups, and there may be no difference in sorption isotherms among samples with three different M/G ratios.

Concluding remarks

The sorption isotherms and permeation of water vapor in films AGA, AGNa and AGCo are not affected by difference in M/G ratios. Great differences, however, are recognized in these behavior among AGA, AGNA and AGCo on the following three points;

(1) The amount of water at sorption equilibrium for AGNa is much higher than that for AGA, while that for AGCo is almost the same as that for AGNa in the region below $p/p_0=0.65$ but is lower above 0.65.

(2) The mean permeability coefficient $\bar{P}(C)$ for AGNa is higher than that for AGA in the whole pressures studied. $\bar{P}(C)$ for AGCo is much lower than that for AGA at lower pressures and it appoaches to that for AGA in the higher pressure region.

(3) No difference is observed in $\bar{D}(C)$ between H_2O-AGA and H_2O-AGNa systems at the same concentrations. In contrast to this, $\bar{D}(C)$ for AGCo is much lower than that for AGA.

In our samples, the G1, M1 and NB films have different M/G ratios, but their crystal parts are mainly composed of poly G. To make the great difference in properties among samples with different M/G ratios, higher content of M-or G-rich samples should be prepared.

If divalent ions with higher affinity in ion exchange reaction than Co are used, for example Cu, there might be any difference among films with different M/G ratios in sorption and permeation properties.

Recently susceptibility of alginate-cobalt complex films to moisture was investigated to explore the practicability for use as a humidity sensor.[20] The catalytic activities for reactions such as decomposition of hydrogen peroxide[21] and oxidation of hydroquinone[22] by the alginate-copper (II) complex membernes were also reported. The fundamental knowledge of the sorption and permeation behavior of water vapor or organic solvents in alginate

samples should be indispensable to develope an application field as mentioned above.

ACKNOWLEDGEMENTS

We wish to thank following researchers of this Institute: Professor Akiyoshi Kawaguchi, Mr. Masayoshi Ohara, and Mr. Shyozo Murakami for X-ray measurements and for helpful discussions; Professor Sorin Kihara and Dr. Yoshiki Sohrin, for their help in the atomic absorption analysis; Professor Seiji Isoda, for valuable discussions.

REFERENCES

1) A. Haug, B. Larsen, and O. Smidsrød, *Carbohydr. Res.*, **32**, 217 (1974), related references therein.
2) E. D. T. Atkins, W. Mackie, and E. E. Smolko, *Nature*, **225**, 626 (1970).
3) E. D. T. Atkins, W, Mackie, K. D. Parker, and E. E. Smolko, *J. Polym. Sci., Part B, Polymer Letters*, **9**, 311 (1971).
4) A. Hirai and H. Odani, to be published.
5) T. Graham, *Phil. Mag., S.4*, **32**, 401 (1866).
6) J. Crank, "The Mathematics of Diffusion," 2nd Ed., Clarendon Press, Oxford, 1975.
7) C. E. Rogers, in "Physics and Chemistry of the Organic Solid State," Vol.2, D. Fox, M. L. Labes, and A. Weissberger Eds., John Wiley & Sons, Inc., New York, 1965, Chap. 6.
8) H. Fujita, *Fortschr. Hochpolym. -Forsch.*, **3**, 1 (1961).
9) H. Grasdalen, B. Larsen, and O. Smidsrød, *Carbohydr. Res.*, **56**, C11 (1977).
10) H. Grasdalen, B. Larsen, and O. Smidsrød, *Carbohydr. Res.*, **89**, 179 (1981).
11) H. Kawarada, A. Hirai, H. Odani, T. Iida, and A. Nakajima, *Polymer Bull.*, **24**, 551 (1990).
12) S. Brunauer, "The Adsorption of Gases and Vapors, Vol I Physical Adsorption," Oxford Univ. Press, Oxford, 1945, p.150.
13) D. Cozzi, P. G. Desideri, and L. Lepri, *J. Chromatogra.*, **40**, 130 (1969).
14) R. A. A. Muzzarelli, "Natural Chelating Polymers," Pergamon Press, New York, 1973, pp29-38.
15) For example, H. Odani, S. Kida, M. Kurata, and M. Tamura, *Bull. Chem. Soc. Japan*, **34**, 571 (1961).
16) E. D. T. Atkins, I. A. Nieduszynski, W. Mackie, K. D. Parker, and E. E. Smolko, *Biopolymers*, **12**, 1865 (1973).
17) E. D. T. Atkins, I. A. Nieduszynski, W. Mackie, K. D. Parker, and E. E. Smolko, *Biopolymers*, **12**, 1879 (1973).
18) E. Frei and R. D. Preston, *Nature*, **196**, 130 (1962).
19) E. D. T. Atkins, W. Mackie, and E. E. Smolko, *Nature*, **225**, 626 (1970).
20) H. Yajima, T. Miyamoto, R. Endo, and S. Furuya, *Kobunshi Ronbunshu*, **46**, 577 (1989).
21) T. Uragami, N. Niwa, and M. Sugihara, *Kobunshi Ronbunshu*, **39**, 669 (1982).
22) T. Uragami, N. Niwa, and M. Sugihara, *Kobunshi Ronbunshu*, **43**, 653 (1986).